

## Diverging Rabi Oscillations in Subwavelength Photonic Lattices

Barak Alfassi, Or Peleg, Nimrod Moiseyev, and Mordechai Segev

*Physics Department and Solid State Institute, Technion, Haifa 32000, Israel*

(Received 6 September 2010; revised manuscript received 21 December 2010; published 14 February 2011)

We show that Rabi oscillations between Bloch modes of an optical waveguide array with subwavelength periodicity diverge, both in frequency and in field amplitude, when the optical wavelength approaches a mathematical exceptional point at which the Bloch mode becomes self-orthogonal.

DOI: 10.1103/PhysRevLett.106.073901

PACS numbers: 42.82.Et, 42.25.Fx, 42.50.Md, 42.70.Qs

Rabi oscillations [1] are known from quantum mechanics, where a two-state system is driven periodically by an electromagnetic (EM) field and undergoes periodic population exchanges. They occur in diverse systems, such as semiconductors [2,3], and Bose-Einstein condensates [4]. Recently, Rabi oscillations were proposed [5] and demonstrated in paraxial photonic lattices [6]: a classical system equivalent in many ways to quantum systems [7]. However, recent technologies make it possible to fabricate structures narrower than the optical wavelength. In such structures, the dynamics must be analyzed through Maxwell equations without approximation. The dynamics in optical nanostructure can be fundamentally different from that in above-wavelength systems, highlighting new phenomena such as form birefringence [8], briefings [9], lower-index guiding [10], optical forces on waveguides [11], enhanced nonlinear effects [12], stimulated Raman amplification [13], and “phoenix solitons” [14].

Here, we study Rabi oscillations between optical Bloch modes in waveguide arrays of subwavelength periodicity. We show that in this realization the Rabi frequency and the electric field of the light diverge as the transition approaches a unique point (known as “exceptional point,” EP) at which one of the optical Bloch modes becomes self-orthogonal. We analyze the influence of back reflections, which eventually govern the dynamics and stop the divergence through a two-stage process. This unusual behavior arises from the structure of Maxwell’s equations, which can give rise to a mathematical EP when the field varies rapidly at subwavelength scale. This phenomenon has no equivalent in quantum systems where the physical potentials are real.

First, we recall concepts related to non-Hermitian operators and EPs. Non-Hermitian operators, which are used to analyze systems with long-lived metastable states, exhibit a unique form of singularity: singularity arising from an EP. At an EP, not only do two sets of eigenvalues coincide, but rather the eigenvectors themselves coalesce [15]. EPs were identified in acoustics [16], microwaves [17], and optical settings such as parity-time symmetric structures [18,19], subwavelength structures [14], and dissipative media [20]. The presence of EP in the spectrum of an operator has physical significance. For example, the

convergence radius of perturbation theory is determined by the EPs, and in parity-time symmetry problems the EP manifests dramatic crossover from an entirely real spectrum to a complex spectrum [21]. At the vicinity of an EP, unique effects can be observed, such as eigenstates exchange, appearance of a nontrivial geometric phase, and mode crossing [17,18,20]. The hallmark of EPs is that, at an EP, two sets of orthogonal eigenstates coalesce into a single eigenstate, which is orthogonal to itself [22]. Hence, mathematically, the wave functions associated with the EP must have infinite amplitudes. Such unique properties of EPs help to explain our results. Let us first derive the existence of an EP in our system.

Our system is a nanoscale waveguide array with high-index contrast. In our recent work [14] we formulated Maxwell’s equations with a non-Hermitian matrix operator  $M(-i\partial_z\varphi = M\varphi)$ . The non-Hermiticity of  $M$  implies evanescent bands, redefined orthogonality relations, and the existence of EPs. Consider a waveguide array, periodic in the  $x$  direction, uniform in  $y$ , and with  $z$  as the propagation direction [Fig. 1(a)]. To induce Rabi oscillations, we later introduce periodic modulations in  $z$  that couple the modes of the structure. Maxwell’s equations in this structure, for TE polarization, time harmonic fields are [14]

$$-i\partial_z \begin{pmatrix} E \\ H \end{pmatrix} = \begin{pmatrix} 0 & -k_0 \\ -\frac{1}{k_0}\partial_x^2 - \varepsilon k_0 & 0 \end{pmatrix} \begin{pmatrix} E \\ H \end{pmatrix} \equiv M\varphi^R, \quad (1)$$

where  $\vec{E} = E\hat{y}$ ,  $\vec{H} = H\hat{x} + H_z\hat{z}$  are the electric and magnetic fields,  $k_0$  is the vacuum wave number, and  $\varepsilon$  the dielectric permittivity. First we treat Eq. (1) as an

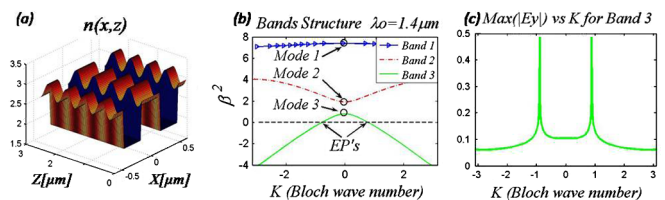


FIG. 1 (color online). (a) Refractive index structure of the waveguide array, displaying the transverse and longitudinal modulations. (b) Band structure for  $d = 0.316 \mu\text{m}$ ,  $\lambda_0 = 1.4 \mu\text{m}$ ,  $n_1 = 2$ ,  $n_2 = 3$ . (c) Maximum amplitude of normalized modes in band 3, showing the amplitude divergence at the EPs.

eigenvalue equation [ $\varphi^R(x, z) = \tilde{\varphi}^R(x)e^{i\beta z}$ ], and find the eigenmodes [23]. We find two sets of eigenvalues, grouped into bands, as expected from a periodic problem  $\varepsilon(x) = \varepsilon(x + D)$ : the forward and backward propagating modes, possessing a positive or negative propagation constant, respectively [Fig. 1(b), with  $K$  normalized by  $1/D$ ]. For either of these modes, as  $\beta^2$  goes below zero, the corresponding mode becomes evanescent, with a pure imaginary propagation constant. When this crossover occurs within a band, the forward and backward propagating bands coincide at the crossover point [Fig. 1(b)]. As we later show, the crossing point is an EP, at which two sets of eigenvalues and eigenvectors coalesce.

We proceed with non-Hermitian tools. We redefine the orthogonality relations via a biorthogonal basis composed of “right” states  $\varphi^R$  [defined by Eq. (1)], and “left” states  $\varphi^L$ —eigenstates of the transposed operator  $M^T$  [21], and labeled  $\varphi_i^L, \varphi_i^R$ . For forward propagating waves

$$\varphi_i^R = \frac{1}{\sqrt{2}} \begin{pmatrix} E_i \\ H_i \end{pmatrix}, \quad \varphi_i^L = -\frac{1}{\sqrt{2}} \begin{pmatrix} H_i^* \\ E_i^* \end{pmatrix}. \quad (2)$$

The norm of an eigenstate according to the biorthogonality relation is  $(\varphi_i^L | \varphi_i^R) = (1/2) \int dx (-H_i^* E_i - E_i^* H_i)$ , having the meaning of the Poynting vector in the propagation direction. Maxwell’s equations yield

$$(\varphi_i^L | \varphi_i^R) = \int \beta |E_i|^2 dx. \quad (3)$$

In the context of self-orthogonality, Eq. (3) proves that if  $\beta = 0$ , its corresponding eigenstate is self-orthogonal. This property is a signature of an EP. Indeed, we find that at the EP two mode coalesce. In this particular case of an EP with EM waves, this result can be also understood intuitively: the difference between a forward and backward propagating wave in the TE polarization is the orientation of the magnetic field, and as  $\beta \rightarrow 0$ ,  $H_x = -(\beta/k_0)E \rightarrow 0$ . Hence, the difference between the forward and backward modes diminishes, until they coalesce at  $\beta = 0$ . Equation (3) implies that, for normalized modes,  $|E(x)| \propto 1/\sqrt{|\beta|}$  [Fig. 1(c)]. Thus, the divergence is not restricted to a singular point, but rather the whole region near the EP diverges. This indicates that self-orthogonality is a physical phenomenon, not just an intriguing mathematical entity. We obtain this result also numerically [Fig. 1(c)].

Next, we study Rabi oscillations between two Bloch modes of a photonic lattice, where one is an ordinary mode and the other is a mode at the vicinity of the EP. Consider a structure in which the EP occurs in band 3 [Fig. 1(b)]. To facilitate Rabi oscillations, the refractive index of the array is also modulated in the propagation direction  $z$ , introducing resonant coupling (Rabi oscillations) between the “lowest” Bloch mode (band 1,  $K = 0$ ) and the  $K = 0$  mode of band 3 (these modes have zero power flow in the  $x$  direction). Light is launched into the lowest Bloch mode—which is far away from the EP. The Rabi oscillations induce periodic energy transfer from

mode 1 to mode 3 [Fig. 1(b)], whose associated eigenvalues are  $\beta_{0,1}, \beta_{0,3}$ . Since the band structure scales with  $\lambda$  ( $k_0 = 2\pi/\lambda$ ), varying  $\lambda$  shifts the EP until it reaches the  $K = 0$  point on band 3. It is hence possible to launch the light into mode 1, and observe the power transferred into a mode 3 that is brought closer and closer to the EP, by varying  $\lambda$  in a continuous fashion. As we later show, only minute changes in  $\lambda$  are needed, so that the “ordinary” excitation mode can effectively remain unchanged.

The periodic modulation of the dielectric permittivity that could couple two such eigenmodes must have a spatial dependence in both  $z$  and the  $x$  [5]. Let us take

$$\varepsilon_p = f(x) \cos(\Delta\beta z), \quad (4)$$

where  $f(x + D) = f(x)$ , and  $\Delta\beta = \beta_{0,1} - \beta_{0,3}$ . This modulation enters the propagation operator as  $-i\partial_z \varphi = [M + V(x) \cos(\Delta\beta z)]\varphi$ ;  $V(x) \equiv \begin{pmatrix} 0 & 0 \\ -k_0 f(x) & 0 \end{pmatrix}$ . Repeating the textbook derivation of Rabi oscillations [5], with the biorthogonality relation defined above yields

$$-i \frac{\partial c_{K', n'}(z)}{\partial z} = \sum_{K, n} c_{K, n}(z) (\varphi_{K', n'}^L | V(x) | \varphi_{K, n}^R) \times [e^{i(\beta_{K, n} - \beta_{K', n'} + \Delta\beta)z} + e^{i(\beta_{K, n} - \beta_{K', n'} - \Delta\beta)z}], \quad (5)$$

where  $c_{K, n}$  is the amplitude of the eigenmode with Bloch momentum  $K$  from band  $n$ . Keeping only phase-matched terms (see discussion below), we find Rabi oscillations  $c_{0,1}(z) = c_{0,1}(0) \cos(\Omega_R z)$ , with the Rabi frequency

$$\Omega_R = |(\varphi_{0,1}^L | V(x) | \varphi_{0,3}^R)| = \left| \int (E_{0,1}^* f(x) E_{0,3}) dx \right|. \quad (6)$$

As the eigenmode  $E_{0,3}$  approaches the EP—its eigenvalue  $\beta$  decreases and approaches zero. As we have shown, the normalized electric field of the mode increases in proportion to  $\beta^{-0.5}$  ( $|E_{0,3}| \propto \alpha \beta^{-0.5}$ ), and thus the Rabi frequency also diverges as  $|E_{0,3}|$  approaches EP:

$$\Omega_R \propto \beta^{-0.5} \xrightarrow{\beta \rightarrow 0} \infty. \quad (7)$$

Thus, both the field and the Rabi frequency—two observable quantities—diverge as power law as the EP is approached. This divergence can be understood as a result of the conservation of energy flux (power) in the  $z$  direction (assuming the absence of back reflections). The modes at the vicinity of the EP are characterized by a very small propagation constant ( $\beta$ ); thus, the energy flux ( $S_z \propto \beta |E|^2$ ) becomes smaller as the EP is approached. Consequently, the conservation of total power requires the divergence of the field amplitude (as the flux is proportional to the properly defined norm, which is also conserved). Such a high field is accomplished through a resonance effect in the  $x$  direction of the array, as a consequence of Bragg reflections (for TM polarization,  $H_y$  will be diverging, while  $E_x$  will be vanishing).

The above analytic derivation has one important assumption: the absence of backscattering [keeping only

phase-matched terms while going from Eqs. (5) to (6). This assumption has direct implications, because backscattering implies that the energy flux along  $z$  is not conserved. The reasoning is that the phase mismatch between the forward and the backward waves is very large, and is not balanced by the modulation in  $z$ . Our simulations below prove the validity of this assumption, as long as we do not get too close to the EP. However, the phase mismatch between the forward and the backward waves becomes smaller as the EP is approached, and is exactly zero at the EP. Hence, the coupling between the forward and the backward propagating waves is what prevents the field amplitude and the Rabi frequency from diverging to infinity. However, exactly at the EP, a two-step process becomes very efficient: first, phase-matched coupling from the forward propagating mode from band 1 to the forward propagating “slow mode” of band 3, and subsequently coupling between the forward propagating mode of band 3 to the backward propagating mode of band 1. This two-step process becomes efficient because its phase mismatch  $2\beta_{03}z$  vanishes when  $\beta_{03} = 0$ . Such a two-step process could prevent the divergence of the modal amplitudes, by providing a channel for power to escape from being trapped in the “slow modes” at the close vicinity of the EP. To investigate this, we later introduce an analytic model accounting for coupling between forward and backward propagation waves. However, as long as we do not get too close to the EP, this “escape mechanism” is not phase matched; hence, the Rabi frequency grows rapidly as  $\Omega_R \propto \beta^{-0.5}$  as the EP is approached.

Next, we simulate the propagation dynamics, including back reflections, by solving Maxwell’s equations with no assumptions. We use the Finite Difference Time Domain code (FDTD) by Rsoft©. In the simulations, the field is launched into the waveguide array at  $z = 0$ , and the periodic modulation of the structure along the propagation direction begins at  $z = 5 \mu\text{m}$ . Our waveguide array has refractive indices of  $n_1 = 2$ ,  $n_2 = 3$ , and period  $D = 632 \text{ nm}$ , giving rise to the band structure of Fig. 1(b). We change the position of the EP in band 3 by varying  $\lambda$ : as  $\lambda$  is increased, the EP moves toward  $K = 0$ , closer to mode 3. We launch mode 1 into the waveguide array at  $z = 0$ . The periodic modulation in  $z$  is on the high-index regions only, with  $\varepsilon_p = 0.3 \cos(\Delta\beta z)$  [Fig. 1(a)], and  $\Delta\beta$ , the modal mismatch, is found numerically. For the chosen parameters, the EP for mode 3 occurs at  $\lambda = 1.521 \mu\text{m}$ .

When mode 3 is far from the EP (for  $\lambda \leq 1.43 \mu\text{m}$ ), the oscillation period is large [ $> 30 \mu\text{m}$ ; Fig. 2(a)]. As we increase  $\lambda$ , the EP moves toward  $K = 0$ , and the oscillation period becomes smaller [ $\lambda = 1.517 \mu\text{m}$ ; Fig. 2(b)]. Clearly, the Rabi frequency is much higher in Fig. 2(b), where mode 3 is closer to the EP. To obtain the Rabi frequency, we project the “instantaneous wave function” onto the eigenmodes during propagation [Figs. 2(c) and 2(d)], using the biorthogonality relation. From the variation of mode 3 along  $z$ , it is clear that its propagation

constant  $\beta_3$  is much lower at  $\lambda = 1.517 \mu\text{m}$  [Fig. 2(d)] than at  $\lambda = 1.43 \mu\text{m}$  [Fig. 2(c)], as expected—since  $E_3 \propto e^{i\beta_3 z}$  (mode 1, being far from the EP, remains practically unchanged when varying  $\lambda$ ). From these projections, we extract the Rabi frequency as a function of  $\lambda$  [Fig. 2(e)]. As shown by the simulations (red dots) and the analytic curve (blue line), the frequency diverges as  $\beta^{-0.5}$ , exactly as predicted by our analytics. We emphasize that this frequency rising is achieved without changing the amplitude of the periodic modulation  $V$ ; hence, it is a direct outcome of the anomaly at the EP where the corresponding mode is self-orthogonal. This simulation proves that back reflections do not affect the results even when the eigenmodes are extremely close to the EP ( $\beta_{0,3} = 0.1$ ). The main result [Eq. (7)] is therefore proved analytically and numerically (Fig. 2): the Rabi frequency and field amplitude diverge with  $1/\sqrt{\beta}$ , as the EP is approached.

These FDTD simulations are sufficiently remote from the EP where backscattering is negligible. However, as we get closer to the EP, simulation time grows rapidly, rendering FDTD impractical. To explore the dynamics in the limit  $\beta_{0,3} \rightarrow 0$ , we introduce an analytic model based on coupled mode theory [24], which also includes the backward propagating waves (denoted by “-” in Eq. (5)). The first forward propagating mode evolves as

$$-i \frac{\partial c_{01}^+(z)}{\partial z} = c_{0,3}^+(z)(\varphi_{0,1}^{+L}|V(x)|\varphi_{0,3}^{+R}) + c_{0,1}^-(z) \times (\varphi_{0,1}^{+L}|V(x)|\varphi_{0,3}^{-R})e^{-i(2\beta_{0,3})z} \quad (8)$$

The second term is negligible for  $\beta_{0,3} > 2\Omega_R$ , because the power exchange with the backward propagating wave

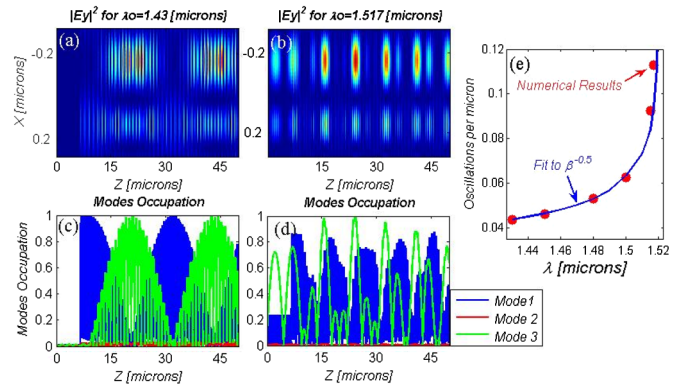


FIG. 2 (color online). Rabi oscillations between two modes associated with different bands of the waveguide array. (a), (b) Field intensity at one unit cell for  $\lambda = 1.43 \mu\text{m}$  and  $\lambda = 1.517 \mu\text{m}$ , respectively. The Rabi oscillations in (a) are the slow variations. The fast oscillations reflect the short effective wavelength inside the medium, not power transfer to mode 3; they arise because the FDTD code yields the intensity at a specific time (not the time-average intensity). (c), (d) Projections of the propagating wave on Bloch modes 1, 2, 3 as a function of  $z$ , for  $\lambda = 1.43 \mu\text{m}$  and  $\lambda = 1.517 \mu\text{m}$ . (e) Analytic (solid line) and simulated (red dots) results displaying the oscillation frequency divergence with  $1/\sqrt{\beta}$  dependence.

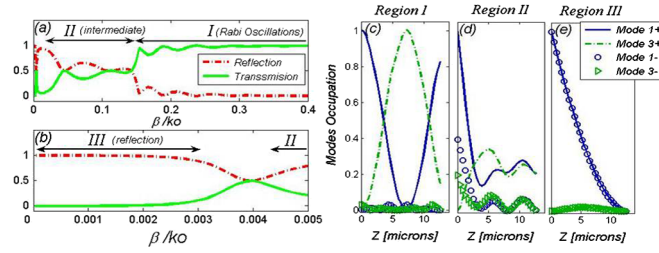


FIG. 3 (color online). (a),(b) Total transmission and reflection as a function of  $\beta_{0,3}$ , for a coupling modulation length of  $L = 13 \mu\text{m}$ . Bottom panel is zoom-in around  $\beta_{0,3} = 0$  of the upper one. The figures reveal three distinct regimes. (I) All the power is transmitted; reflections are negligible. (II) Reflection becomes significant. (III) Entire incident wave is back reflected. (c),(d), (e) Propagation dynamics in each one of the regimes of (a),(b). (c)  $\beta_{0,3} = 0.3k_0$ : Rabi oscillations between mode 1+ and mode 3+, while reflected waves are negligible. (d)  $\beta_{0,3} = 0.1k_0$ : intermediate regime, where reflections affect the dynamics, but oscillations between the modes still occur. (e)  $\beta_{0,3} = 0.001k_0$ : all the incident wave (mode 1+) is reflected back (to mode 1-).

( $\propto \Omega_R$ ) is much slower than the mismatch term ( $\propto \beta_{0,3}$ ). However, for  $\beta_{0,3} < 2 \cdot \Omega_R$  this term must be included. To find the full dynamics, we solve four coupled equations like Eq. (7), for each one of the amplitudes  $c_{0,1}^+$ ,  $c_{0,3}^+$ ,  $c_{0,1}^-$ ,  $c_{0,3}^-$ , coupling term  $\varepsilon_p = \begin{cases} f(x) \cos(\Delta\beta \cdot z); & 0 < z < L \\ \text{else} \end{cases}$ . Figures 3(a) and 3(b) display the total transmission  $T \equiv |c_{0,1}^+(L)|^2 + |c_{0,3}^+(L)|^2$  and the total reflection  $R \equiv |c_{0,1}^-(0)|^2 + |c_{0,3}^-(0)|^2$ , as a function of  $\beta_{0,3}$ , for  $L = 13 \mu\text{m}$ , under boundary conditions  $c_{0,1}^+(0) = 1$ ,  $c_{0,3}^+(0) = 0$ ,  $c_{0,1}^-(L) = 0$ ,  $c_{0,3}^-(L) = 0$ , which properly describes launching mode  $c_{0,1}^+$  from  $z < 0$  into the system. Figures 3(a) and 3(b) reveal three distinct regimes. For  $\beta_{0,3} > 0.15k_0$  (regime I;  $\beta_{0,3} > 2 \cdot \Omega_R$ ), back reflections are negligible ( $R = 0$ ,  $T = 1$ ), while Rabi oscillations between  $c_{0,1}^+$ ,  $c_{0,3}^+$  diverge as  $1/\sqrt{\beta_{0,3}}$  [Fig. 3(c)]. For  $0.004k_0 < \beta_{0,3} < 0.15k_0$  (regime II), back reflections affect the dynamics dramatically [Fig. 3(d)]: the oscillations no longer behave as Rabi oscillations. For example, the phase between  $c_{0,1}^+$ ,  $c_{0,3}^+$  is not  $\pi/2$ , the dynamics is sensitive to the modulation length  $L$ , and the oscillation frequency does not diverge as  $\beta_{0,3}^{-0.5}$ . Finally, for  $\beta_{0,3} < 0.004k_0$  (regime III), reflections govern the dynamics: power exchange between the modes vanishes, and the entire incident wave is back reflected [ $R = 1$ ,  $T = 0$ ; Fig. 3(e)]. This dynamics is similar to Bragg reflection by a two-stage process where modes 3,  $c_{0,3}^+$  acts as mediator between  $c_{0,1}^+$  and  $c_{0,1}^-$ .

Under the parameters of Fig. 3, the optical intensity grows by a factor of 10 as the EP is approached, before back reflections prevail. Such growth in intensity is easily observable experimentally by controlling a single “knob”: continuous variation of  $\lambda$  with a tunable laser. However, this “maximum growth” value is not a fundamental limit: the maximal intensity value can be dramatically increased through parameters optimization, e.g., by reducing the

coupling factor  $f(x)$  between the Bloch modes. This will reduce  $\Omega_R$ , allowing one to get closer and closer to the EP before back reflections become dominant, hence experiencing larger enhancements of the field amplitude.

To conclude, we studied optical Rabi oscillations in subwavelength waveguide arrays, at the proximity of a mathematical EP, and find that the oscillation frequency and field amplitude diverge as the EP is approached. This feature is unique to Rabi oscillations in optical systems, as described by Maxwell equations. We find that small changes in the optical wavelength can dramatically affect the dynamics, offering an effective tool for light manipulation in nanostructures, and can be used to switch on or off nonlinear effects in a selective fashion. Last but not least, the Rabi frequency can be used as an experimental observable, to show that self-orthogonality involves observable phenomena, allowing one to study the vicinity of the EP in great detail. This work raises an interesting question: is it possible to find an enhancement of the Rabi frequency in a quantum system that supports an EP?

This work was supported by an Advanced ERC Grant. B. A. is grateful to the Azrieli Foundation for support.

- [1] I. I. Rabi, *Phys. Rev.* **49**, 324 (1936).
- [2] A. Schulzgen *et al.*, *Phys. Rev. Lett.* **82**, 2346 (1999).
- [3] J. R. Petta *et al.*, *Science* **309**, 2180 (2005).
- [4] M. R. Matthews *et al.*, *Phys. Rev. Lett.* **83**, 3358 (1999).
- [5] K. G. Makris *et al.*, *Opt. Express* **16**, 10 309 (2008).
- [6] K. Shandarova *et al.*, *Phys. Rev. Lett.* **102**, 123905 (2009).
- [7] F. Lederer *et al.*, *Phys. Rep.* **463**, 1 (2008).
- [8] F. Xu *et al.*, *Opt. Lett.* **20**, 2457 (1995).
- [9] I. Richter *et al.*, *Appl. Opt.* **34**, 2421 (1995).
- [10] Q. Xu *et al.*, *Opt. Lett.* **29**, 1626 (2004).
- [11] A. Mizrahi and L. Schächter, *Phys. Rev. E* **70**, 016505 (2004); *Opt. Express* **13**, 9804 (2005); M. Pivellini *et al.*, *Appl. Phys. Lett.* **85**, 1466 (2004)
- [12] V. R. Almedia *et al.*, *Nature (London)* **431**, 1081 (2004).
- [13] R. Espinola *et al.*, *Opt. Express* **12**, 3713 (2004).
- [14] O. Peleg *et al.*, *Phys. Rev. Lett.* **102**, 163902 (2009).
- [15] W. D. Heiss, *Eur. Phys. J. D* **7**, 1 (1999); *Phys. Rev. E* **61**, 929 (2000).
- [16] A. L. Shuvalov *et al.*, *Acta Mech.* **140**, 1 (2000).
- [17] C. Dembowski *et al.*, *Phys. Rev. Lett.* **86**, 787 (2001).
- [18] K. G. Makris *et al.*, *Phys. Rev. Lett.* **100**, 103904 (2008).
- [19] C. E. Rüter *et al.*, *Nature Phys.* **6**, 192 (2010).
- [20] S. Lee *et al.*, *Phys. Rev. Lett.* **103**, 134101 (2009).
- [21] C. M. Bender and S. Boettcher, *Phys. Rev. Lett.* **80**, 5243 (1998); S. Klaiman, U. Günther, and N. Moiseyev, *Phys. Rev. Lett.* **101**, 080402 (2008).
- [22] N. Moiseyev and S. Friedland, *Phys. Rev. A* **22**, 618 (1980); E. Narevicius, P. Serra, and N. Moiseyev, *Europhys. Lett.* **62**, 789 (2003).
- [23] P. Yeh, A. Yariv, and C.-S. Hong, *J. Opt. Soc. Am.* **67**, 423 (1977).
- [24] See supplemental material at <http://link.aps.org/supplemental/10.1103/PhysRevLett.106.073901> for details on the analytic model.